Inequality of nitrogen use and loss in global croplands caused by climate change

Chenchen Ren
Zhejiang University
Xiuming Zhang
The University of Melbourne https://orcid.org/0000-0002-1961-3339
Stefan Reis
UK Centre for Ecology & Hydrology https://orcid.org/0000-0003-2428-8320
Jiaxin Jin
Hohai University
Jianming Xu
Zhejiang University https://orcid.org/0000-0002-2954-9764
Baojing Gu (bjgu@zju.edu.cn)
Zhejiang University https://orcid.org/0000-0003-3986-3519

Article

Keywords:

Posted Date: December 2nd, 2021

DOI: https://doi.org/10.21203/rs.3.rs-1066140/v1

Abstract

Maintaining food production while reducing agricultural pollution is a grand challenge under the threats of global climate change, which has exerted negative impacts on agricultural sustainability. How agricultural nitrogen use and loss respond to climate change is rarely understood. Here we show that climate change leads to inequality of cropland nitrogen use and loss across global regions based on historical data for the period 1961-2018 from 143 countries. Increases of yield, nitrogen surplus and nitrogen use efficiency (NUE) are identified in 30% of countries, while reductions are observed for the remaining 70% of countries, as a result of climate change. Farm size changes further intensify the inequality of nitrogen use and pollution in global croplands. Yet, enlarging farm size can facilitate climate change adaptation, by which global cropland NUE could be increased by one-third in 2100 compared to 2018 under future shared socioeconomic pathways. Our results would be of great significance to sustain global agriculture as well as eliminate national inequalities on food production and agricultural pollution control.

Full Text

Global climate change has led to an increase in both average ambient temperatures observed and the frequency of extreme weather events, including dry-hot and precipitation extremes [1–3]. These changes not only threaten human and ecosystem health, but also adversely affect agricultural production [4, 5]. Mitigating the negative impacts of climate change on agriculture is a grand challenge, in the context of safeguarding food security for a growing and increasingly wealthy global population.

Nitrogen (N) fertilizer use has fed about half of the global population [6]; however, N use in croplands has exceeded the safe planetary boundary, leading to substantial environmental problems such as air and water pollution, biodiversity loss, soil acidification and global warming (ozone layer depletion and nitrous oxide (N_2O) emission) [7, 8]. Currently, over 100 million tonnes of fertilizer N is applied to global croplands annually and over half of the N is lost to the environment, leading to an average N use efficiency (NUE) below 50%, a critical indicator for agricultural sustainability [8, 9]. So far, climate change impacts have been rarely considered when developing management strategies for sustainable agricultural N use, as the focus has been primarily on the climate effects of N fertilizer use, such as N_2O emissions [10]. Yet, climate change can affect agricultural N use and losses, for instance, and warming temperatures can increase ammonia emissions from croplands [11, 12]. The warming climate has been shown to aggravate N pollution in Australia [13].

Here, we quantified the impact of climate change (annual mean temperature, annual precipitation and their quadratic terms) on global crop yield (in terms of N harvested including all crop species), fertilization (total N fertilizer use on croplands), N surplus (N not harvested by crop) and NUE (N harvested by crop divided by total N input). To understand the interaction between climate change and agricultural practices on cropland N use and loss, farm size is introduced to represent changes in agricultural practices [14].

Large-scale farming typically indicates a different management scheme compared to smallholder farming, with improved knowledge and farming facilities [14]. A panel model is used for the analysis of past-counterfactual scenarios (1961-2018) and predicting future trends (towards the year 2100) based on future Shared Socioeconomic Pathways (SSP) scenarios (more details see Methods).

Results And Discussion

Spatial variability under climate change

The average air temperature increased across regions worldwide from 1961 to 2018 (Fig. 1 and S1), varying from 0.36 ºC (Latin America) to 2.28 ºC (Former Soviet Union). The average air temperature in the high and middle latitudes of the Northern Hemisphere is generally lower than that in the remaining regions. However, the temperature increase is more significant in these colder regions, especially in North America and the Former Soviet Union. These variations in averages and changes lead to variability in N use and loss between croplands in different world regions.

Over the period from 1961 to 2018, global NUE changes on average by an annual decline of 0.2% (Fig. 2g), with large variations between colder countries in the high and middle latitudes of the Northern Hemisphere and warmer countries in low latitudes and the Southern Hemisphere (Fig. 3g). NUE increases were noted in about 30% of countries worldwide with an average value at 3% (1-11%) in the single year 2018 due to global warming, which mainly distributed in warmer countries in the high and middle latitudes of the Northern Hemisphere. But for more than 70% of countries with a colder climate in the low latitudes and the Southern Hemisphere, rising temperatures have reduced the NUE by 4% (0-10%).

Warming contributes to the NUE increase as a result of yield increases at the same time as fertilization reduction, such as observed in Canada and Russia. There was an increase of 0-5% (averaged at 2%) in yield in 7% of countries worldwide in the single year 2018 (Fig. 3a, Extended Data Fig. 1), which are all located in the high latitudes of the Northern Hemisphere, where a slight cooling has occurred. Meanwhile, the N fertilization rate declined globally due to global warming, with an average of 8% and substantial variations across countries from 3% (Bangladesh) to 22% (Sweden) (Fig. 2d, Fig. 3d). In Russia, Canada and some Scandinavian countries in the high latitudes of the Northern Hemisphere, large temperature variations have made the average N fertilization declined by around 20% in 2018. In contrast, NUE reduces in the remaining 70% of warmer countries due to global warming. One of the most important reasons is that most of these countries have a much larger proportion of yield loss even with the reduced fertilization, such as in Australia. Crop yield declined by about 7.1% (3-13%) in these countries due to temperature increases in 2018 (Fig. 3a, Extended Data Fig. 1). However, the N fertilization rate reduced less, only averaged at 5.8% (3-10%). These different responses to climate change lead to national inequalities on agricultural N use that further cascades to the variability of food production and environmental quality.

Unexpectedly, N surplus has been decreasing since 1961 with climate warming even with yield and NUE reductions (Fig. 2a, g, j), indicating a reduction in excess N application. This is mainly due to the larger proportion of fertilization reduction on a global scale, compared to yield decline (Fig. 2a and 2d). Spatially, N surplus declined by 4% (0-26%) in 70% of countries worldwide in 2018 due to climate warming, with hotpots distributed in the high and middle latitudes of the Northern Hemisphere (Fig. 3j). In comparison, N surplus increased 6% (0-12%) in the rest 30% global countries, mainly distributed in the low latitudes and the Southern Hemisphere. For instance, in Canada and Russia, the N surplus has been reduced by more than 20% in 2018. But at the same time, N surplus also increased in Brazil and Central Africa with an average of 10%.

Crop yield, fertilization, NUE and surplus have changed slightly after taking precipitation into analysis, especially for N fertilization (Fig. 2). In 2018, precipitation only led to approximately 0.2%, 0.04%, 0.2%, and 0.2% changes in global yield, fertilization, NUE and surplus, respectively (Fig. 3). But the combined impact of temperature and precipitation has further enhanced the spatial variability of N use and loss.

Non-linear response to climate change

The primary mechanism driving the spatial variability of N use and loss can be attributed to non-linear responses of key parameters to climate change. Air temperature change relates to crop yield following an inverted-U shape (Table 1, Extended Data Fig. 2) and the turning point is calculated at approximately 6.6 ºC (Extended Data Table 1). Temperature near the turning point is beneficial to reach a high crop yield. In countries with an average temperature below 6.6 ºC, warming will increase crop yield, such as in Canada, Russia and countries in the high latitudes of the Northern Hemisphere. But when the temperature exceeds the turning point, there will be a negative effect on crop yield, for example, countries from the low latitudes and Southern Hemisphere. The higher the temperature increase, the larger the yield loss. There is a U-shape relationship between temperature and fertilization with a turning point at approximately 59 ºC that is hard to be reached (Table 1 and Extended Data Table 1). It means current air temperature increase would significantly reduce fertilization across all countries.

The non-linear responses of yield and fertilization caused by temperature changes further affect cropland NUE. An inverted-U shape between temperature and cropland NUE is observed with the turning point at 10 ºC. For most countries in the high and middle latitudes of the Northern Hemisphere, global warming is expected to contribute to an NUE increase given their average temperature is before the turning point. In contrast, global warming is projected to reduce NUE in warmer countries since their temperature has passed the turning point. Meanwhile, N surplus has typically an opposite change with NUE and yield, with a U shape with climate warming with the turning point at 14 ºC.

While there are no clear trends for precipitation at a global scale, large variations are projected for different years. The effect of precipitation on yield and NUE is similar to temperature following an inverted-U relationship (Table 1, Extended Data Fig. 2). It indicates that precipitation in a moderate range (about 2,500 mm of annual precipitation) is beneficial to yield and NUE (Extended Data Table 1). However, extreme precipitation events (far away from the turning point, too much or too little precipitation) and their spatial variability usually lead to floods and droughts, which could substantially reduce agricultural yield and cropland NUE. Consequently, N surplus shows a U-shaped relationship with precipitation considering there is no significant relationship between precipitation and N fertilization (Table 1). Specifically, excess N application could be lowered in the range of moderate precipitation (about 2,400 mm of annual precipitation) but would surge under extreme precipitations (Extended Data Table 1).

Moderate temperature and precipitation can benefit crop yield, which is partly attributed to an increase in photosynthesis. Extremes in temperature and precipitation could destroy the growth environment of crops and then lowered their yields. Global warming often causes dry and hot extremes at the same time [3], which leads to farmers reducing fertilizer input to cropland as the average temperature rising. Irrigation can alleviate the negative impact of yield and fertilization caused by global warming [15, 16]. But there are still gaps for irrigation to compensate for these adverse effects [16, 17]. Thus, it can still be observed that temperature rising reduces agricultural N yield and fertilization even we take the impact of irrigation into consideration (Table 1). In addition to fertilizer and yield, climate change also affects the NUE in other pathways. For example, climate change increases N losses from croplands by aggravating gas emissions such as NH_3 [18]; extreme rainfall intensifies soil erosion, taking away N in cropland soil and reducing NUE [19]. Climate change may also play a critical role in the rate of biological N fixation [20, 21].

Farm size changes intensify spatial variability

Farm size shows a positive correlation with cropland NUE and N yield, but negative with N fertilization and surplus (Table 1). Global average farm size has declined since 1961 mainly due to the increase of rural population, with a 38% reduction in 2018 compared to the 1961 level (Extended Data Fig. 3a). The decline was sharp in the early decades but has since slowed down, especially in the period after the 1990s. As a result, global cropland NUE has been further reduced compared to that under climate change effects, despite the trend easing after the 1990s (Fig. 2g, h, i). Similarly, crop yield is further reduced, and N fertilization and surplus are rebounded affected by changes in farm size (Fig. 2c, f, l). In contrast, farm size has increased in about 30% of countries globally, including China, Russia, most South American and Europe countries (Extended Data Fig. 3b). N yield and NUE improvements, and N fertilization and surplus reductions can be found for these countries (Fig. 3c, f, i, l).

Climate change reductions in crop yield are offset by an increase in farm size in China, which also leads to a decrease in fertilizer use by 15%, NUE improvement by 6% and N surplus declines by 5%. In the Netherlands, Norway and Finland, NUE increases by 17% on average due to farm size increase. Unfortunately, the reduction in farm size in most countries has aggravated the negative impacts of climate change, especially in Africa, Middle East, Oceania and some Southeast Asian countries. Crop yield loss has been further increased from 8–21% due to farm size decline in Sub-Saharan Africa. Similar results can be observed in fertilization from decrease 7% to increase 16%, leading to NUE reduced to 21% from 6% and N surplus increased to 17% from 2% in 2018. Generally, farm size changes further improved NUE in Asian and European countries in middle and high latitudes and reversed NUE reduction in Latin

American countries in the southern hemisphere. However, reduction of cropland NUE in the remaining countries in low latitudes and Southern Hemisphere was aggravated and the positive effects of climate change on NUE were weakened in North America.

There is diverging performance between small- and large-scale farms regarding N use and loss under climate change conditions. NUE changes due to changes in climate tend to be much smaller on large-scale farms (> 2 ha) compared to small-scale farms (≤ 2 ha) (Fig. 4a, b), indicating a higher degree of vulnerability of smallholders from climate change. Large-scale farming in contrast contributes to higher crop N yield, while reducing N fertilization, leading to NUE improvements and a reduction in N surplus. Meanwhile, measures to enable adaptation to climate change are different for large and small-scale farms, illustrated by the interactions we find between farm size and climate change (Table 1).

To quantify the relative contribution of climate change effects and farm size on N use and losses in global croplands, we estimated the standardization coefficient of the explanatory variables in both small- and large-scale farms for the period 1961 to 2018 (Fig. 4c, d). Results show that effect from farm size change towards large-scale farms can reverse the declining trend of NUE and crop yield, which reduce N losses. The effect from farm size change is much smaller in small-scale farms compared to that in the large-scale farms. Analyzing the combined effects of climate change and farm size, a reduction of NUE and crop yield are still found in small-scale farms, albeit at a smaller scale, which may be due to the substantial reduction of N fertilizer use with climate change in small-scale farms.

Large-scale farms usually have better infrastructure, including drainage and irrigation facilities, which can improve NUE while maintaining or increasing crop yield [22, 23]. Better knowledge of large-scale farmers benefits their ability to adapt to climate change to minimize negative impacts. In contrast, smallholders are vulnerable to climate change due to a lack of agricultural facilities and knowledge. In this paper, we used harvested N per ha to represent crop yield, which is positively correlated to farm size. It may be interpreted as the result of improved seeds, more targeted N fertilizer application, scientific and technologically supported farm management and advanced technology under large-scale farming. However, these effects can vary substantially across global regions (Extended Data Fig. 4). The negative effect of temperature on NUE is much larger in Africa than that in most other regions, and farm size also has a negative effect on NUE due to the decline of farm size there with increase of rural population. In contrast, farm size has a much larger positive effect on NUE, which even reduces the negative impact from climate change due to the better facilities and farmer knowledge from the large-scale farms in North America.

Enlarging farm size would offset climate impact

Global average NUE changes under different SSP scenarios would remain stable if only temperature increases are considered (Extended Data Fig. 5). However, substantial spatial variability further diverges between colder countries in the high and middle latitudes of Northern Hemisphere and warmer countries in low latitudes and the Southern Hemisphere in 2100. Even under the optimum scenario (SSP1) with a projected temperature increase by 3.0 ℃ by 2100 compared to pre-industrial level, yield and NUE would be further reduced in warmer countries in low latitudes and Southern Hemisphere compared to the observed in 2018 (Fig. 5, Fig. S2). Yield decreases are averaged at 8% projected for 95% of countries globally in 2100, mainly distributed in low latitudes and Southern Hemisphere. NUE decline will be further aggravated, especially in Africa, South and Southeast Asia and Latin America (Extended Data Fig. 6).

In contrast, increase projected in North America and Former Soviet Union would strengthen their already high NUE and yield, which will exacerbate the national inequalities on agricultural N use and loss. A further temperature increase presents a barrier to further reducing the global input of N fertilizer between -5% and -22% compared to 2018. N surplus will further worsen in the Southern Hemisphere, aggravating N pollution in Australia and Brazil while reducing N surplus of some Scandinavian countries (Fig. 5, Extended Data Fig. 6). In the worst-case scenario (SSP3) with global average temperature increasing by 4.1 ℃ in 2100, theses impacts would be diverging more seriously globally (Extended Data Fig. 7, Fig. S3). It will substantially change the current pattern of N use, aggravating the inequalities on food production and agricultural environmental protection.

Enlarging farm size is a critical path for climate adaptation to ensuring food security and reduce agriculture pollution while eliminating their national inequalities. In the optimum (SSP1) scenario, the global average urbanization rate will exceed 90% by 2075 and reach up to 93% by 2100. That means that a large number of the rural population will move to urban areas, leading to the increase of average farm size due to consolidation of many smallholder farms into fewer large-scale farms [24]. As a result, large-scale farming will reverse the declining trend of cropland NUE over time, projected to increase from 44% in 2018 to 59% in 2100, with a 21% yield increase and 35% decline of N surplus (Extended Data Fig. 5). More importantly, the spatial variability of NUE changes due to global warming could be balanced through enlarging farm size with NUE improvements across all countries (Fig. 5) and eliminating the national inequalities.

Even in the SSP3 scenario with an average urbanization rate of only 70% in 2100, the global average NUE also increases to 47% (Extended Data Fig. 5), including the effect of farm size change. However, the yield will decrease slightly by 0.2%, and N surplus will decline by 13%. That is mainly due to the unbalanced development leading to the diverging trends of farm size across different countries. In developing regions such as Africa, South and southeast Asia, average farm sizes would decline substantially. This will result in more yield and NUE reduction, then increase N surplus. In sub-Saharan Africa, NUE decreases by an average of 25% and N surplus increases by 17% in 2100 compared to 2018 (Extended Data Fig. 7, Fig. S3). In contrast, the average farm size will further increase in developed regions such as North America, Europe and Oceania. The declining trends of crop yield and NUE due to rising average temperature would be reversed through enlarging farm size.

Enlarging farm size reduces spatial variability on agricultural N use and loss caused by climate change and reduce national inequalities under SSP1 scenario. Promoting sustainable N use by increasing farm size involves multiple stakeholders, including government, farmers, social organizations etc. [25]. For example, establishing an N credit system for these stakeholders presents a viable path to improve NUE and reduce N losses [26]. Urbanization is also having a profound impact on the release of more croplands and reduction of rural population, which in turn will benefit large-scale farming [24, 27]. Moreover, training and better agricultural facilities and technologies are also effective measures to enable adaptation to the adverse effects of climate change [28]. Improving cropland NUE and managing agricultural land sustainably would in turn slow down the rise in temperature rising reduction of greenhouse gas emission from agriculture [29, 30]. Thus, early actions should be taken to ease the projected future impact of climate change on agriculture to achieve the global sustainable goals [31, 32].

Methods

Data sources and data processing. Data used in this study are mainly collected from the Food and Agriculture Organization online statistical databases of the United Nations (FAOSTAT) (http://www.fao.org/statistics/databases/en/). FAOSTAT provides comprehensive and standardized agricultural and socioeconomic data all over the world from 1961 to the most recent year available. In this paper, the calculation of cropland fertilization and yield, NUE, cash crop ratio, agricultural land area per rural population (proxy variable of farm size), and the gross domestic product per capita (PGDP) are based on agricultural production, fertilization (including synthetic fertilizer and manure), irrigation, land use, population, and so on.

The average country-level farm size data is derived from Lowder et al., 2014 [33]. It is the average of farmers' actual operating agricultural land area. In this paper, agricultural land area per rural population was adopted as the proxy variable of farm size due to data limitation. The relationship of the farmland area per rural population and the actual farm size is listed in Table S1 to show the rationality of this replacement.

Dataset for global inorganic N deposition at a spatial resolution of 2° × 2.5° was derived from Ackerman et al., 2019 [34]. Information on global irrigation management was derived from the FAO's Global Information System on Water and Agriculture (http://www.fao.org/aquastat/en/).

Historical observations of climatic data, including the mean air temperature, total precipitation, and atmospheric carbon dioxide (CO_2) concentration, were considered in our analysis. The monthly temperature (°C) and precipitation (mm/month) from January 1961 to December 2018 were derived from the Centre for Environmental Data Analysis (CEDA) global climatic dataset at 0.5° × 0.5° spatial resolution (Available online: http://badc.nerc.ac.uk). The Atmospheric Infrared Sounder (AIRS) monthly carbon dioxide concentration (ppm) at a spatial resolution of 2.5° × 2° from September 2002 to February 2017 was derived from the Goddard Earth Sciences Data and Information Services Center (GES DISC) (Available online: https://disc.gsfc.nasa.gov/). For each selected country, the climatic variables were sampled by nearest neighbor assignment according to the boundary and averaged by month.

And we also obtained the counterfactual monthly climate data with and without climate change from Ortiz-Bobea et al., 2021 [35]. Data are fully provided at the Cornell Institute for Social and Economic Research (CISER): https://doi.org/10.6077/pfsd-0v93. We averaged their monthly bias-corrected data of seven general circulation models (GCMs) from the "hist-nat' and the 'historical' experiment as weather data with and without climate change, respectively.

We obtained country-level rural population and average global temperature increase data based on the Shared Socioeconomic Pathways (SSP) database hosted by the IIASA Energy Program (https://tntcat.iiasa.ac.at/SspDb). The country-level rural population was obtained to calculate farm size. Farm size and temperature changes under different SSP scenarios are presented in Extended Data Fig. 8. In this paper, we only consider three SSP scenarios with low (SSP1), intermediate (SSP2), and high developing challenges (SSP3), respectively.

Nitrogen budget. This study compiled the global cropland N budgets at a national scale from 1961 to 2018 based on the Coupled Human And Natural Systems (CHANS) model. CHANS is a N mass balance model which combines bottom-up N input and output fluxes among 14 subsystems (cropland, livestock, grassland, forest, aquaculture, industry, human, pet, urban green land, wastewater treatment, garbage treatment, atmosphere, surface water, and groundwater) and top-down reactive N fluxes datasets on different (regional, national, global) scales to provide a comprehensive understanding of N cycling and fluxes [36]. A detailed model introduction can be found in Zhang et al., 2017 [37] and Gu et al., 2015 [36]. In this study, the cropland system is identified as the subject in CHANS, the calculation of cropland N budget in each country is formulated in Eq. (1-3):

$$N_{input,\,i} = N_{fer,\,i} + N_{man,\,i} + N_{fix,\,i} + N_{dep,\,i} + N_{irr,\,i}$$

1

$$N_{output,\,i} = N_{harvest,\,i} + N_{gas,\,i} + N_{runoff,\,i} + N_{leaching,\,i}$$

2

$$NUE_i = \frac{N_{harvest,\,i}}{N_{input,\,i}}$$

3

where $N_{input,\,i}$ is the total N inputs to the cropland across all crops in the country *i*, include synthetic fertilizer application ($N_{fer,\,i}$), manure application ($N_{man,\,i}$), biological fixation ($N_{fix,\,i}$), atmospheric deposition ($N_{dep,\,i}$), and irrigation ($N_{irr,\,i}$). $N_{output,\,i}$ is the total N outputs from the cropland, include crop harvest ($N_{harvest,\,i}$, the sum of the yield of each crop multiplied by their N content), N gas emissions ($N_{gas,\,i}$, including NH_3, N_2, N_2O and NO_x emissions), riverine runoff ($N_{runoff,\,i}$), and leaching to groundwater ($N_{leaching,\,i}$). The estimates of different N outputs from croplands are based on parameters and emission factors nested in the CHANS model. NUE (NUE_i) is defined as the ratio of harvest N to total N inputs in cropland system in country *i*. Accordingly, we derived yield (kg N ha^{-1}) in each country using crop harvest N divided by the total harvest area. And fertilization (kg N ha^{-1}) is the ratio of the sum of N content in synthetic fertilizer application to the total harvest area. Surplus (kg N ha^{-1}) is the difference between the harvest N and total N inputs of the cropland system per area.

Statistical analysis. To estimate the response of agricultural N yield, fertilization, NUE and surplus to climate change and farm size changes, we used a fixed-effect model to do panel analysis while controlling for compounding factors such as cash crop ratio and irrigation. We estimated the following equation using country-level data from 1961 to 2018:

$$Ln\,Y_{it} = \alpha + \beta \cdot Ln\,Farmsize_{it} + \gamma_1 \cdot T_{it} + \gamma_2 \cdot T_{it}^2 + \delta_1 \cdot P_{it} + \delta_2 \cdot P_{it}^2 + \theta_1 \cdot Ln\,Farmsize_{it} \cdot T_{it} + \theta_2 \cdot Ln\,Farmsize_{it} \cdot T_{it}^2 + \theta_3 \cdot Ln\,Farmsize_{it} \cdot P_{it} + \theta_4 \cdot Ln\,Farmsize_{it} \cdot P_{it}^2 + \sum_n \varphi_n q_{nit} + \sigma_i + \mu_{it} \tag{4}$$

where the subscript *i* and *t* denotes country and year, respectively. Y_{it} are explained variables, namely, yield, fertilization, NUE and N surplus. $LnFarmsize$ is the logarithm of the agricultural land area per rural population. T and P are the abbreviations of the average temperature (10^2 °C) and accumulative precipitation (10^4 mm) across the year, respectively. T^2 and P^2 are their quadratic terms. We also introduced the interaction items of T, P, T^2 and P^2 with $LnFarmsize$ to explore the role of farm size under climate change. q_n is control variable, including cash crop ratio, irrigation, country code and year. In the equations whose explained variable is yield, NUE and N surplus, fertilization is further controlled. α is a constant, σ_i and μ_{it} are error items. $\beta,\ \gamma,\ \delta,\ \theta and \phi$ are coefficients that need to be estimated. The cash crop ratio is the harvest area of cash crops divided by the total harvest area. Irrigation is a binary variable (equaling to 1 and 0 if there is or no irrigated land, respectively). Interaction items have been centered by each year group when doing regression analysis to make regression coefficient more practical. We did the regression analysis in Stata16.0 software. The regression results are detailed in Table 1 and summary statistics are in Table S2.

Note that we consider the annual precipitation (summed by monthly precipitation) and average temperature (averaged by monthly temperature) across the year rather than growing seasons as representing climate change. This is mainly because that yield, fertilization, NUE and N surplus are calculated based on a country-level cropland system incorporating multiple crops that grow in almost all months.

Impact of climate change and farm size. We calculated the impact of global warming (GW), climate change (CC) by subtracting the predicted value under the weather with climate change from the predicted value under the weather without climate change. The weather data with and without climate change were averaged from seven GCMs [10]. The combined impacts of climate and farm size change (CFSC) were further assessed, assuming the farm size remains unchanged from 1961. For country *i*, the predicted value (with or without climate and farm size changes) is calculated according to:

$$LnY_{it} = \alpha + \beta \bullet LnFarmsize_{it} + \gamma_1 \bullet T_{it} + \gamma_2 \bullet T_{it}^2 + \delta_1 \bullet P_{it} + \delta_2 \bullet P_{it}^2 + \sum_n \phi_n q_{nit} + \sigma_i + \mu_{it}$$

5

where the subscript i and t denotes country and year, respectively. Y_{it} are explained variables, namely, yield, fertilization, NUE and N surplus. $LnFarmsize$ is the logarithm of the agricultural land area per rural population. T and P are the abbreviations of the average temperature (10^2 °C) and accumulative precipitation (10^4 mm) across the year, respectively. T^2 and P^2 are their quadratic terms. α is a constant, σ_i and μ_{it} are error items. The coefficients β, γ, δ have been estimated. q_n is control variable including cash crop ratio, irrigation, country code, and year. In the equations whose explained variable is yield, fertilization is further controlled. In the equations whose explained variable is NUE, fertilization and yield are both controlled. Based on coefficients estimated in Eq. (7), we calculated the impacts on each country as follows:

$$Impact_{it}^{GW} = \exp\left(LnY_{it}^{Observed} + LnY_{it}^{WithoutGW} - LnY_{it}^{WithGW}\right) - Y_{it}^{Observed}$$

(6)

$$Impact_{it}^{CC} = \exp\left(LnY_{it}^{Observed} + LnY_{it}^{WithoutCC} - LnY_{it}^{WithCC}\right) - Y_{it}^{Observed}$$

(7)

$$Impact_{it}^{CFSC} = \exp\left(LnY_{it}^{Observed} + LnY_{it}^{WithoutCFSC} - LnY_{it}^{WithCFSC}\right) - Y_{it}^{Observed}$$

(8)

Note that we first derived the impact on fertilization. Then yield was derived based on predicted fertilization as it is one of the explanatory variables. NUE was derived based on predicted fertilization and yield. The impact of N surplus was finally calculated, which is the difference between predicted harvest N and total N input then divided by harvest area. Predicted harvest N is derived N yield multiplying harvest area. Total N input was derived according to N yield and NUE based on Eq. (3). When we calculated the country-level impact in the year 2018, the relative changes depicted in Fig. 3 were derived. When the country-level impact from 1961 to 2018 was calculated, the weighted global mean was showed in Fig. 2. N yield, fertilization and surplus were weighted by national harvest area. And NUE was weighted by total cropland N input in each country.

To reflect the joint statistical uncertainty from the econometric model and climate uncertainty, we calculated the impacts for 5,000 random pairs of bootstrapped coefficients for Eq. (7). The spatial patterns of physical impacts and the upper and lower limits are in Extended Data Fig. 1, Fig. S4 and S5, respectively.

Scenario analysis. We considered three SSP scenarios (SSP1, SSP1, and SSP3 with low, intermediate, and high developing challenges, respectively) to conduct scenario analyses to see how the agricultural yield, fertilization, NUE and N surplus would change if global warming and farm size changes continue. SSP1 is the sustainable and "green" pathway with high urbanization and reduced national economic inequalities, which the global temperature will increase 3.0℃ by 2100 compared to the pre-industrial level. SSP2 is the "middle of the road" or medium pathway extrapolating the past and current global development into the future. Income trends in different countries are diverging significantly and global population growth is moderate. The global temperature increase will be up to 3.8 ℃ by 2100. Under SSP3, a revival of nationalism and regional conflicts pushes global inequality to rise. Global population growth is the largest among these three scenarios. And the global temperature increase will be up to 4.1 ℃ by 2100. The temperature and farm size changes under SSPs are depicted in Extended Data Fig. 8.

First, we obtained country-level rural population and average global temperature increase data (2005-2100) from the SSP database. And we assumed the total area of agricultural land remains unchanged from 2018 and calculated country-level agricultural land area per rural population by the ratio of the agricultural land area to the rural population from 2020 to 2100. Then we got the changes of agricultural land area per rural population compared to 2018. Meanwhile, the average global temperature increase has been converted to increase compared to 2018 and was adopted as country-level temperature increase. In this process, we compared the global average temperature increase from 2005 to 2010 and rural population data from CEDA and FAOSTAT, respectively, with the data from the SSP database. Accordingly, we weighted the scenario temperature increase and rural population proportionally to reduce the error caused by different databases. Then the yield, fertilization, NUE and N surplus trend were derived based on Eq. (7) as follows:

$$\Delta LnY_{it}^{SSP} = \beta \bullet \Delta LnFarmsize_{it} + \gamma_1 \bullet \Delta T_{it} + \gamma_2 \bullet \Delta T_{it}^2$$

9

$$Y_{it}^{SSP} = \exp\left(LnY_{i,2018}^{Observed} + \Delta LnY_{it}^{SSP}\right)$$

(10)

Note that Δ refers to the value difference between year *i* and 2018.

Similarly, we first derived the impact of fertilization. Then yield was derived based on predicted fertilization as it is one of the explanatory variables. NUE was derived based on predicted fertilization and yield. The impact of N surplus was finally calculated, which is the difference between the predicted harvest N and total N input then divided by harvest area. Predicted harvest N is derived N yield multiplying harvest area. Total N input was derived according to N yield and NUE based on Eq. (3). Note that global means of N yield, fertilization and surplus were weighted by national harvest area. And global average NUE was weighted by total cropland N input in each country. The relative changes of N yield, fertilization, NUE and N surplus in 2100 under SSP1, SSP2 and SSP3 are in Fig. 5, Extended Data 5 and Fig. S6, respectively. The physical changes under SSP1, SSP2 and SSP3 are in Fig. S2, S3 and S7, respectively.

Declarations

Data availability

Data supporting the findings of this study are available within the article and its supplementary information files. All data are publicly available and open access.

Acknowledgements

This study was supported by the National Natural Science Foundation of China (42061124001, 41822701 and 41773068).

Author contributions

B.G. designed the study. C.R. conducted the research. B.G., and C.R. wrote the first draft of the paper, X.Z., and S.R. revised the paper. X.Z., and J.X. processed the raw data. And all authors contributed to the discussion and revision of the paper.

Declaration of competing interest

All authors have no conflicts of interest to report.

References

1. Revel, D. Climate change 2014: synthesis report. (Veille énergie climat, 2014).
2. Kirchmeier-Young, M.C. & Zhang, X. Human influence has intensified extreme precipitation in North America. *Proc. Natl. Acad. Sci. U. S. A.* **117**, 13308-13313 (2020).
3. Alizadeh, M.R., *et al.* A century of observations reveals increasing likelihood of continental-scale compound dry-hot extremes. *Sci. Adv.* **6**, z4571 (2020).
4. Xu, C., Kohler, T.A., Lenton, T.M., Svenning, J. & Scheffer, M. Future of the human climate niche. *Proc. Natl. Acad. Sci. U. S. A.* **117**, 11350-11355 (2020).
5. Zhao, C., *et al.* Temperature increase reduces global yields of major crops in four independent estimates. *Proc. Natl. Acad. Sci. U. S. A.* **114**, 9326-9331 (2017).
6. Erisman, J.W., Sutton, M.A., Galloway, J., Klimont, Z. & Winiwarter, W. How a century of ammonia synthesis changed the world. *Nat. Geosci.***1**, 636–639 (2008).
7. Steffen, W., *et al.* Planetary boundaries: Guiding human development on a changing planet. *Science* **347**, 1259855 (2015).

8. Zhang, X., *et al*. Managing nitrogen for sustainable development. *Nature* **528**, 51–59 (2015).
9. Oene, O., *et al*. Nitrogen Use Efficiency (NUE) - an indicator for the utilization of nitrogen in agriculture and food systems Prepared by the EU Nitrogen Expert Panel (2015).
10. Reay, D.S., *et al*. Global agriculture and nitrous oxide emissions. *Nat. Clim. Chang.* **2**, 410–416 (2012).
11. Sutton, M.A., *et al*. Towards a climate-dependent paradigm of ammonia emission and deposition. *Philos. Trans. R. Soc. B-Biol. Sci.* **368**, 20130166 (2013).
12. Huang, X., *et al*. A high-resolution ammonia emission inventory in China. *Glob. Biogeochem. Cycle* **26**, B1030 (2012).
13. Sun, Y., *et al*. The Warming Climate Aggravates Atmospheric Nitrogen Pollution in Australia. *Research* 2021, 1-12 (2021).
14. Ren, C., *et al*. Fertilizer overuse in Chinese smallholders due to lack of fixed inputs. *J. Environ. Manage.* **293**, 112913 (2021).
15. Zaveri, E., Russ, J. & Damania, R. Rainfall anomalies are a significant driver of cropland expansion. *Proc. Natl. Acad. Sci. U. S. A.* **117**, 10225-10233 (2020).
16. Wang, X., *et al*. Global irrigation contribution to wheat and maize yield. *Nat. Commun.* **12**, 1235 (2021).
17. Higginbottom, T.P., Adhikari, R., Dimova, R., Redicker, S. & Foster, T. Performance of large-scale irrigation projects in sub-Saharan Africa. *Nat. Sustain.* **4**, 501–508 (2021).
18. Tian, H., *et al*. Global soil nitrous oxide emissions since the preindustrial era estimated by an ensemble of terrestrial biosphere models: Magnitude, attribution, and uncertainty. *Glob. Change Biol.* **25**, 640–659 (2019).
19. Tan, Z., *et al*. Increased extreme rains intensify erosional nitrogen and phosphorus fluxes to the northern Gulf of Mexico in recent decades. *Environ. Res. Lett.* **16**, 54080 (2021).
20. Rousk, K., Sorensen, P.L. & Michelsen, A. What drives biological nitrogen fixation in high arctic tundra: Moisture or temperature? *Ecosphere* **9**, e2117 (2018).
21. Gundale, M.J., Nilsson, M., Bansal, S. & Jäderlund, A. The interactive effects of temperature and light on biological nitrogen fixation in boreal forests. *New Phytol.* **194**, 453–463 (2012).
22. Castellano, M.J., Archontoulis, S.V., Helmers, M.J., Poffenbarger, H.J. & Six, J. Sustainable intensification of agricultural drainage. *Nat. Sustain.* **2**, 914–921 (2019).
23. Wang, J., Klein, K.K., Bjornlund, H., Zhang, L. & Zhang, W. Adoption of improved irrigation scheduling methods in Alberta: An empirical analysis. *Can. Water Resour. J.* **40**, 47–61 (2015).
24. Wang, S., *et al*. Urbanization can benefit agricultural production with large-scale farming in China. *Nat. Food* **2**, 183–191 (2021).
25. Pretty, J., *et al*. Global assessment of agricultural system redesign for sustainable intensification. *Nat. Sustain.* **1**, 441–446 (2018).

26. Gu, B., *et al*. A Credit System to Solve Agricultural Nitrogen Pollution. *The Innovation* **2**, 100079 (2021).
27. Gu, B., Zhang, X., Bai, X., Fu, B. & Chen, D. Four steps to food security for swelling cities. *Nature* **566**, 31–33 (2019).
28. O Neill, B.C., *et al*. The effect of education on determinants of climate change risks. *Nat. Sustain.* **3**, 520–528 (2020).
29. Roe, S., *et al*. Contribution of the land sector to a 1.5°C world. *Nat. Clim. Chang.* **9**, 817–828 (2019).
30. Mayer, A., Hausfather, Z., Jones, A.D. & Silver, W.L. The potential of agricultural land management to contribute to lower global surface temperatures. *Sci. Adv.* **4**, q932 (2018).
31. Wei, Y., *et al*. Self-preservation strategy for approaching global warming targets in the post-Paris Agreement era. *Nat. Commun.* **11**, 1624 (2020).
32. Hoegh-Guldberg, O., *et al*. The human imperative of stabilizing global climate change at 1.5°C. *Science* **365**, w6974 (2019).
33. Lowder, S.K., Skoet, J. & Singh, S. What do we really know about the number and distribution of farms and family farms worldwide? Background paper for The State of Food and Agriculture 2014. *ESA Working Paper No. 14-02. Rome, FAO.* (2014).
34. Ackerman, D., Millet, D.B. & Chen, X. Global Estimates of Inorganic Nitrogen Deposition Across Four Decades. *Glob. Biogeochem. Cycle* **33**, 100–107 (2019).
35. Ortiz-Bobea, A., Ault, T.R., Carrillo, C.M., Chambers, R.G. & Lobell, D.B. Anthropogenic climate change has slowed global agricultural productivity growth. *Nat. Clim. Chang.* **11**, 306–312 (2021).
36. Gu, B., Ju, X., Chang, J., Ge, Y. & Vitousek, P.M. Integrated reactive nitrogen budgets and future trends in China. *Proc. Natl. Acad. Sci. U. S. A.* **112**, 8792-8797 (2015).
37. Zhang, X., *et al*. Ammonia Emissions May Be Substantially Underestimated in China. *Environ. Sci. Technol.* **51**, 12089–12096 (2017).

Table

Table 1 | Regression results of yield, fertilization and NUE under climate change

	Ln Yield	Ln Fertilization	Ln NUE	Ln Surplus
Ln Farm size	0.14***	-0.36***	0.14***	-0.10***
Temperature	1.76**	-12.82***	3.93***	-2.76*
Temperature^2	-13.35***	19.11**	-16.58***	9.00**
Precipitation	3.62***	0.38	3.67***	-2.54***
Precipitation^2	-9.35***	-1.62	-9.69***	6.68***
Temperature×Ln Farm size	0.67	8.18***	-1.19*	-1.34
Temperature^2×Ln Farm size	0.46	-11.25*	1.93	5.04*
Precipitation×Ln Farm size	0.71***	0.02	1.59***	-1.58***
Precipitation^2×Ln Farm size	-3.56***	-0.84	-5.54***	4.54***
Ln Fertilization	0.08***		-0.12***	0.25***
N	7106	7106	7106	7097
Adjust R^2	0.92	0.86	0.84	0.90
Within R^2	0.15	0.03	0.26	0.31

$^{*}p < 0.05$, $^{**}p < 0.01$, and $^{***}p < 0.001$. Temperature and precipitation are the average temperature (10^2 °C) and accumulated precipitation (10^4 mm) across the year, respectively. Yield is all crop harvest nitrogen (kg ha^{-1}). Fertilization refers to nitrogen fertilization input (kg ha^{-1}). NUE is an abbreviation of nitrogen use efficiency of the agricultural cropland system. Surplus is the difference between the harvest nitrogen and the total input nitrogen (kg ha^{-1}). Cash crop ratio, irrigation, country code, and year effect have been controlled in all regression equations.

Figures

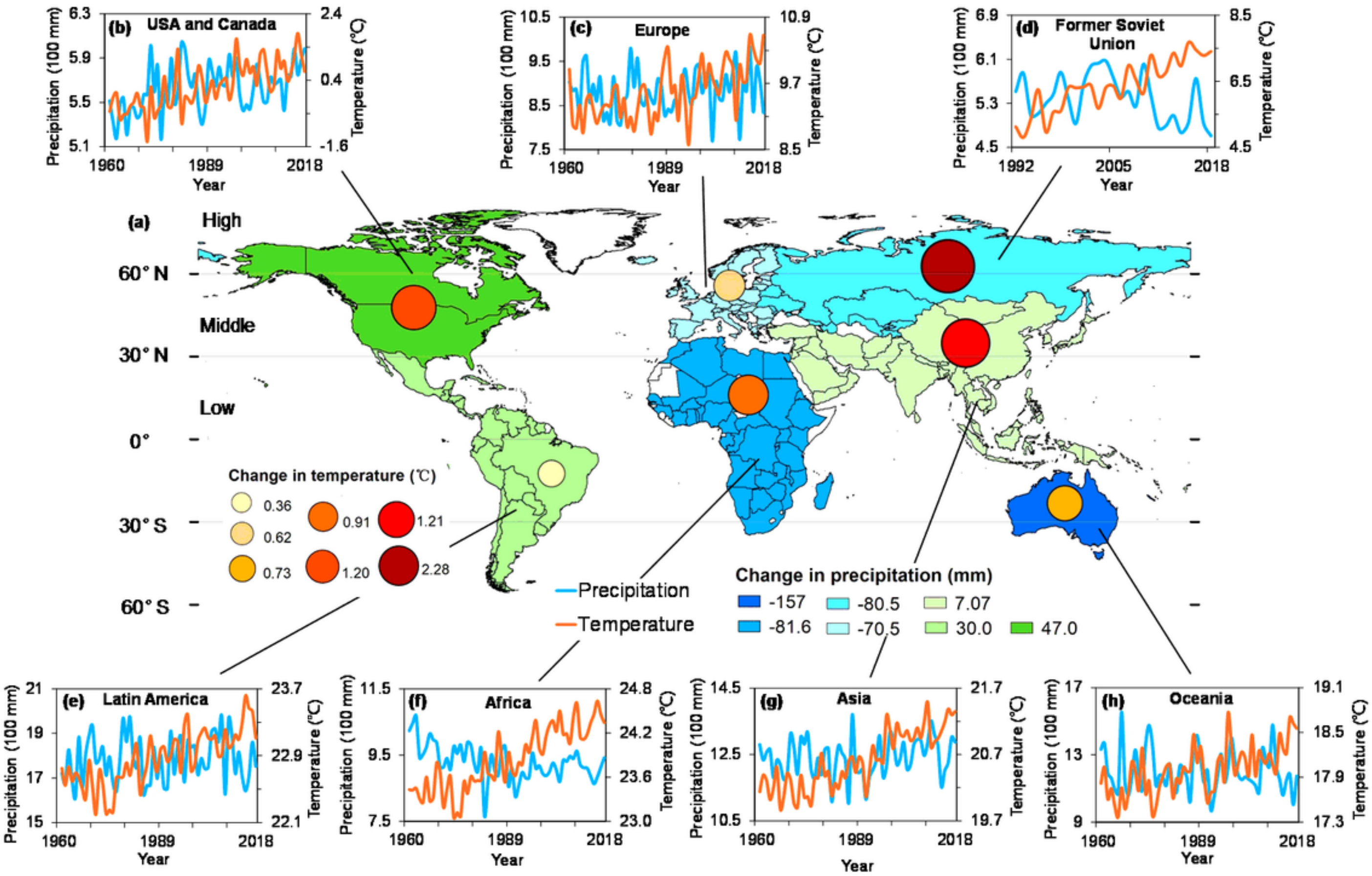

Figure 1

Temperature and precipitation changes across global regions from 1961 to 2018. Panel (a) presents the absolute change of precipitation and temperature between 2018 and 1961. The latitude lines are added in panel (a). Latitudes between 0° and 30°, 30° and 60°, and over 60° are considered low, middle and high latitudes, respectively. The base map is applied without endorsement from GADM data (https://gadm.org/). Panel (b)-(i) illustrate the temporal variation of annual precipitation and average temperature by region, which are shown on the primary and secondary axis, respectively.

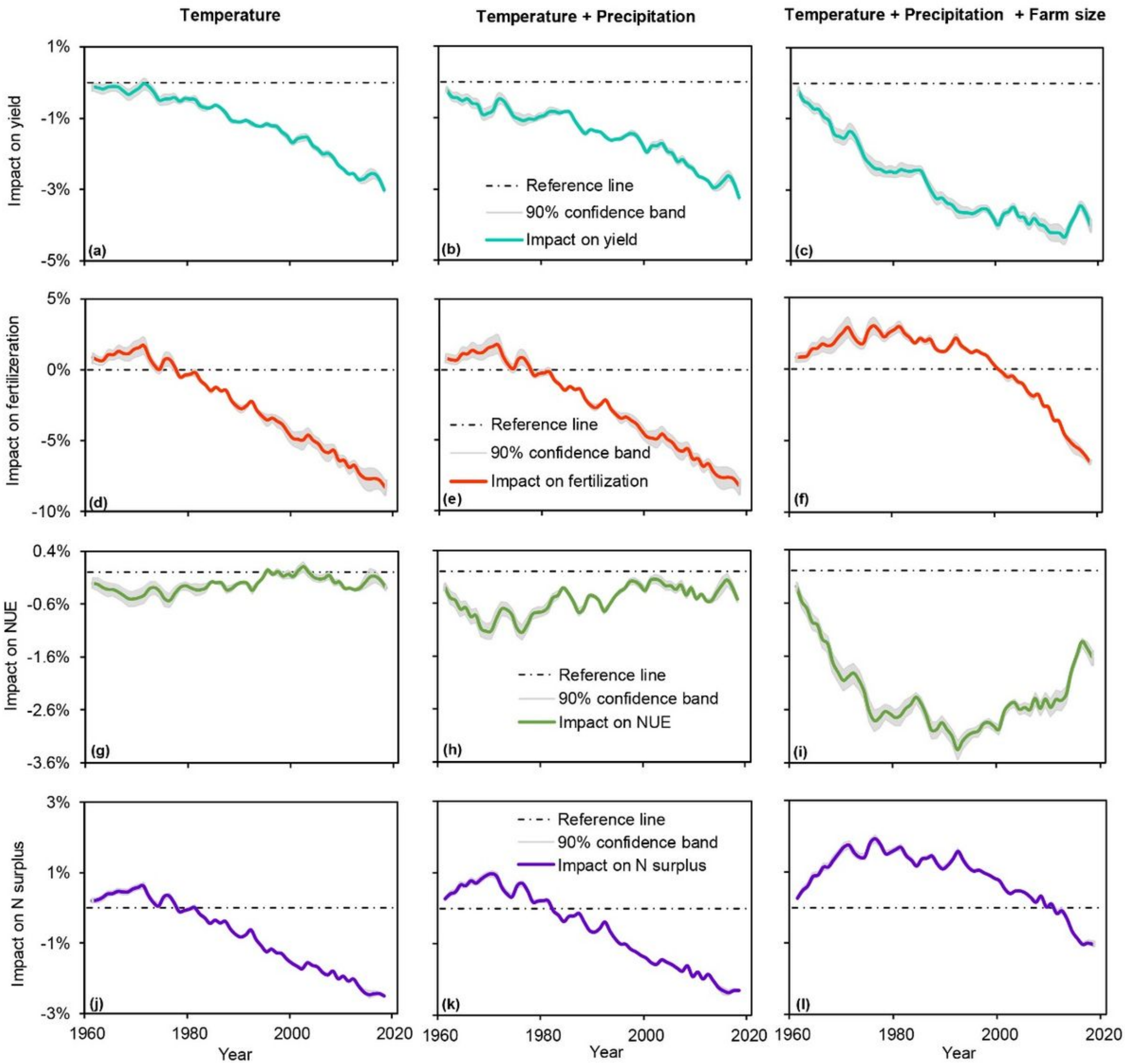

Figure 2

Global impacts of climate and farm size changes on yield, fertilization, NUE and N surplus from 1961 to 2018. (a), (d), (g), and (j) present the impacts of temperature changes on yield, fertilization, NUE, and N surplus, respectively. The impacts of climate change are shown in panels (b), (e), (h), and (k). Combined impacts of temperature, precipitation, and farm size are depicted in panels (c), (f), (i), and (l). The black dotted line is the reference line equaling to zero, indicating that there is no impact, and the grey cone represents a 90% confidence band based on 5,000 bootstraps estimates. In this figure, the global impacts of climate change refer to the relative change (%). It is calculated by value difference predicted under the climate with and without temperature and precipitation changes divided by the observed value in the corresponding year, and the result is carried out in percentage terms. We calculated the combined impacts without climate and farm size changes, assuming the farm size remains unchanged from 1961. All global means in this figure are weighted and taken as a three-year moving average.

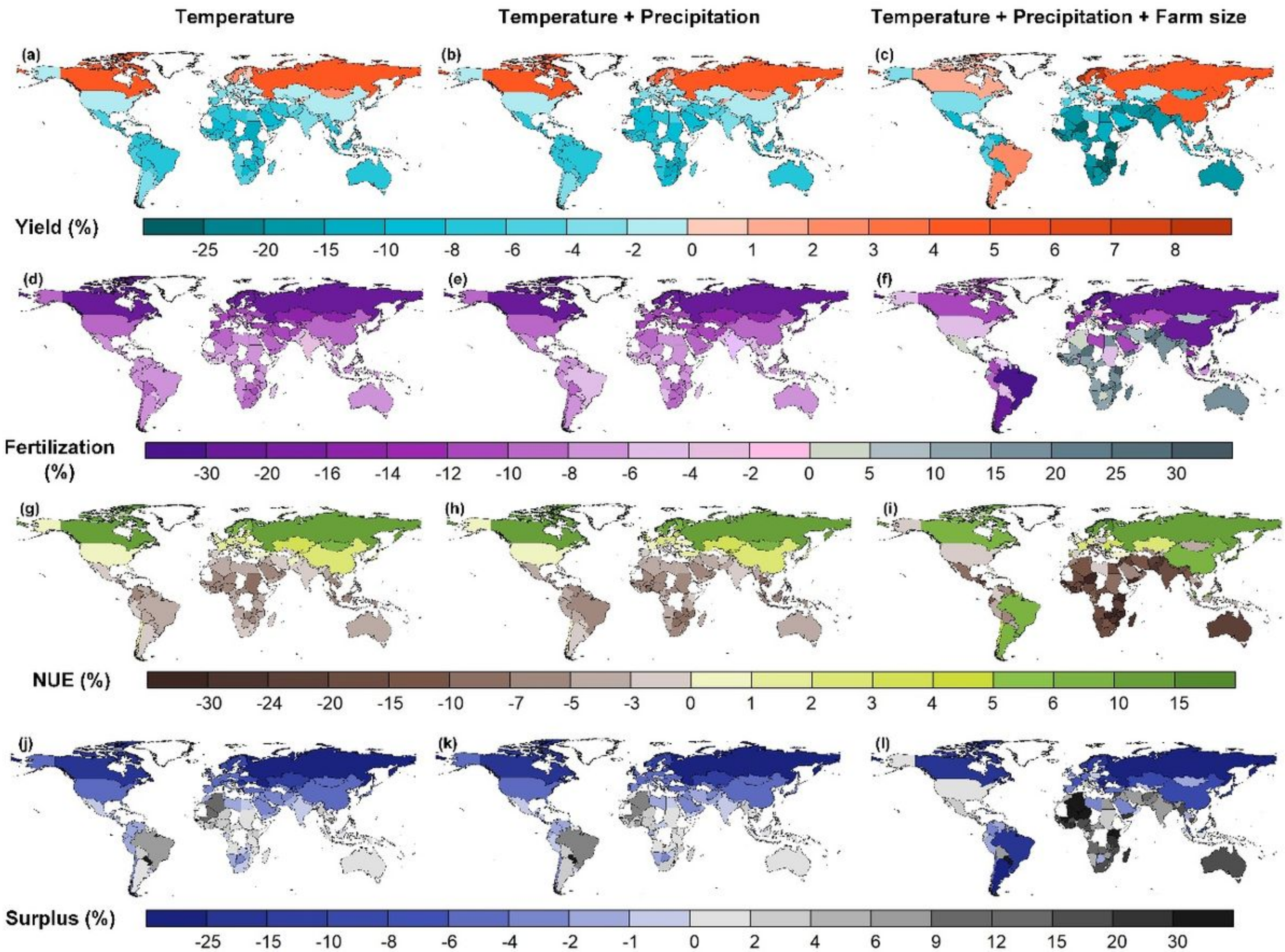

Figure 3

Spatial variability of impact of climate change and farm size on yield, fertilization, NUE and N surplus in 2018. (a), (d), (g), and (j) present the spatial impacts of temperature changes on yield, fertilization, NUE, and N surplus, respectively. The spatial impacts of climate change are shown in panels (b), (e), (h), and (k). Combined impacts of temperature, precipitation, and farm size are depicted in panels (c), (f), (i), and (l). The impact of climate change on each country refers to the relative change (%). It is calculated by the value difference predicted under the climate with and without temperature and precipitation changes divided by the observed value in 2018, and the result is carried out in percentage terms. And we calculate the combined impacts without climate and farm size changes further, assuming the farm size remains unchanged from 1961. The base map is applied without endorsement from GADM data (https://gadm.org/).

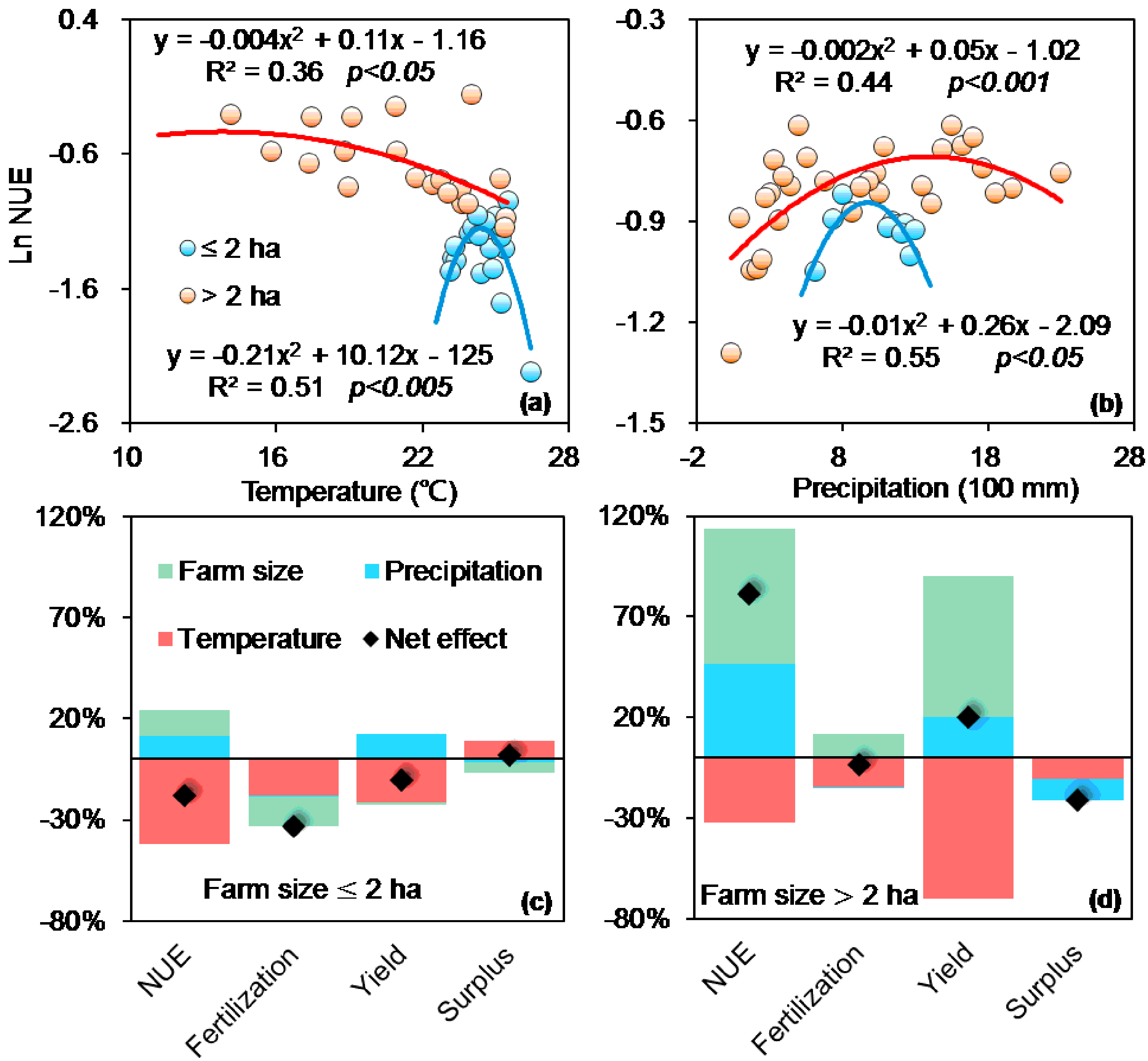

Figure 4

Interaction effect of climate change and farm size on cropland N use and loss. Data of panels (a) and (b) are from Latin America and Africa, respectively. Each data point represents an average value of the log-transformed NUE within a certain farm size and precipitation group (40 groups in total), respectively, which can be found in SI Table S6. Both have been controlled other compounding effects such as cash ratio and fertilization. Panel (c) and (d) show the relative effects of climate change and farm size on NUE, fertilization, yield and N surplus changes among small and large farm size groups (≤ 2 ha and > 2 ha, respectively). The effects were derived from the ratio of the standardization coefficient of each explanatory variable to the standard deviation of the explained variable according to Eq. (7) covering all sample countries from 1961 to 2018. The total effects from temperature and precipitation depicted in panel (c) were summed the effects from themselves and their quadratic items in each farm size group.

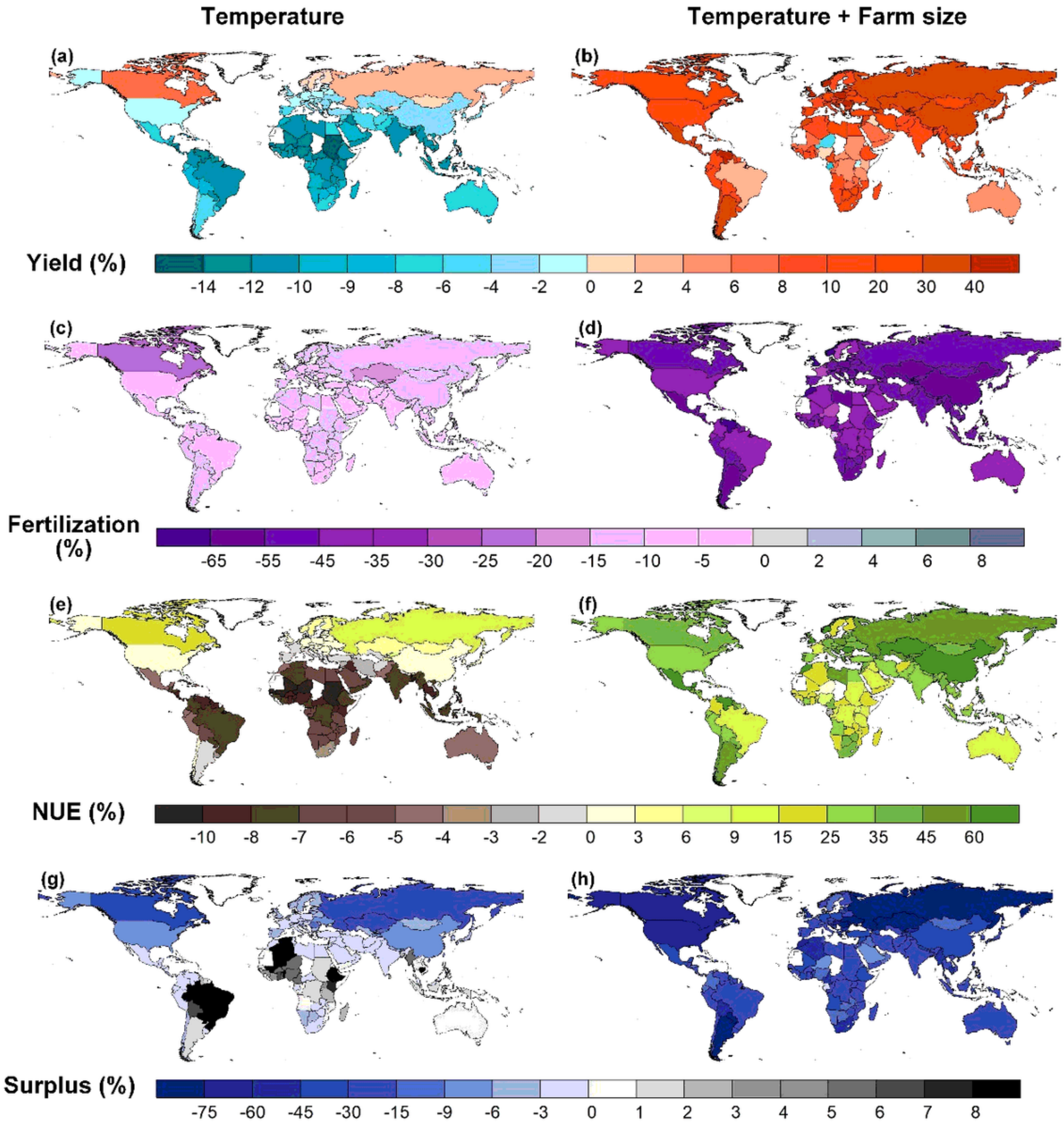

Figure 5

Yield, fertilization, NUE and N surplus changes in 2100 under the optimal SSP scenario (SSP1). Value changes refer to the relative change (%) in this figure. It is calculated by the value difference subtracting the observed value in 2018 from the simulated value in 2100 under the SSP1 scenario divided by the observed value in 2018 and the result is carried out in percentage terms. The left panel shows changes under the SSP1 scenario only considering the temperature. The right panel represents changes further considering the role of farm size. The base map is applied without endorsement from GADM data (https://gadm.org/).

Supplementary Files

This is a list of supplementary files associated with this preprint. Click to download.

- SupplementaryMaterials.docx
- Extendedfigurestables.docx